INTERNATIONAL JOURNAL OF CHEMICAL REACTOR ENGINEERING

Volume 6 2008 *Presentation* P2

Photoreactor Modeling: Applications to Advanced Oxidation Processes

Orlando M. Alfano* Alberto E. Cassano†

*INTEC, Universidad Nacional del Litoral - CONICET, alfano@intec.unl.edu.ar

†INTEC, Universidad Nacional del Litoral - CONICET, acassano@ceride.gov.ar

ISSN 1542-6580

Photoreactor Modeling: Applications to Advanced Oxidation Processes*

Orlando M. Alfano and Alberto E. Cassano

Abstract

A general methodology for photoreactor analysis and design based on the fundamentals of chemical reaction engineering and radiative transfer in participating media is presented. Three applications in the field of advanced oxidation processes are considered to illustrate the proposed approach: (i) a photocatalytic reactor for air purification, (ii) a homogeneous photo-Fenton solar reactor, and (iii) a heterogeneous photocatalytic slurry reactor. In the first case, the procedure is exemplified with the modeling of a multiannular photocatalytic reactor for perchloroethylene removal from contaminated air streams. A rigorous physical and mathematical model of the multiannular concentric photoreactor was developed and experimentally verified. The second approach is illustrated with the degradation of a model pollutant by the Fenton and photo-Fenton reactions in a nonconcentrating, flat-plate solar reactor. Formic acid was chosen as the model substrate. The effect of the reaction temperature on the pollutant degradation rate is analyzed. In the case of the slurry photoreactor, the intrinsic kinetics of the photocatalytic decomposition of a toxic organic compound in aqueous solution, using suspended titanium dioxide catalytic particles and ultraviolet polychromatic radiation, is studied. The kinetic parameters are evaluated for different catalyst loadings, irradiation levels and pollutant initial concentrations. By means of these illustrative examples, the need of a systematic and rigorous approach to the analysis and design of photoreactors is emphasized.

KEYWORDS: photoreactor modeling, advanced oxidation process, pollution remediation, photocatalysis, photo-Fenton, radiation field

---

*The authors are grateful to the Universidad Nacional del Litoral, Consejo Nacional de Investigaciones Científicas y Técnicas, and Agencia Nacional de Promoción Científica y Tecnológica for their support to produce this work. They particularly thank Doctors H.A. Irazoqui, R.J. Brandi, G.E. Imoberdorf, M.L. Satuf, G.H. Rossetti, and Engineers J. Farias and E.D. Albizzati, who have participated in the different original research work that was used to show the chosen applications. The authors also thank Engineer C.M. Romani for technical assistance.

1. INTRODUCTION

The modeling of a conventional reactor based on first principles requires the solution of the momentum, thermal energy, and multicomponent mass conservation equations. In the case of a photoreactor, the photon balance (radiation energy) must be added. The radiation balance can be treated separately from the thermal energy balance because thermal effects of the photochemically useful energy are generally negligible and, consequently, one is mainly concerned with the kinetic effects of the absorbed radiation.

When expressing the rate of a photochemical reaction it is necessary to make the distinction between dark (or thermal) and radiation activated steps. To treat the dark reactions one uses the same methodology as for conventional reactors; the main difference appears when evaluating the rate of the radiation activated step. The existence of this very particular step constitutes the main distinctive aspect between thermal and radiation activated reactions. The rate of the radiation activated step is proportional to the absorbed, useful energy through a property that has been defined as the Local Volumetric Rate of Photon Absorption, LVRPA (Cassano et al., 1995) or the Local Superficial Rate of Photon Absorption, LSRPA (Imoberdorf et al., 2005). The LVRPA represents the amount of photons that are absorbed per unit time and unit reaction volume and the LSRPA the amount of photons that are absorbed per unit time and unit reaction surface.

The general structure of the problem may be described as indicated in Figure 1. The mass balances ask for expressions formulating the reaction rates; always some of the steps are initiated by radiation absorption. The radiation activated step kinetics is always written in terms of the photon absorption rate (the LVRPA or the LSRPA). The evaluation of the photon absorption rate is performed stating first the Radiative Transfer Equation (RTE) that requires the appropriate constitutive equations for radiation absorption, emission and scattering (Section 2). Boundary conditions for the RTE must account for the existence of UV lamps and reflectors (or direct and diffuse radiation for solar reactors) and the effects of the reactor walls (for example, wall transmittance and fouling of the radiation entrance window). The resulting RTE is then successively applied to the reaction space for a nonparticipating medium (Section 3), for a homogeneous medium where there is only radiation absorption (Section 4), and for a heterogeneous medium where there are radiation absorption and scattering (Section 5).

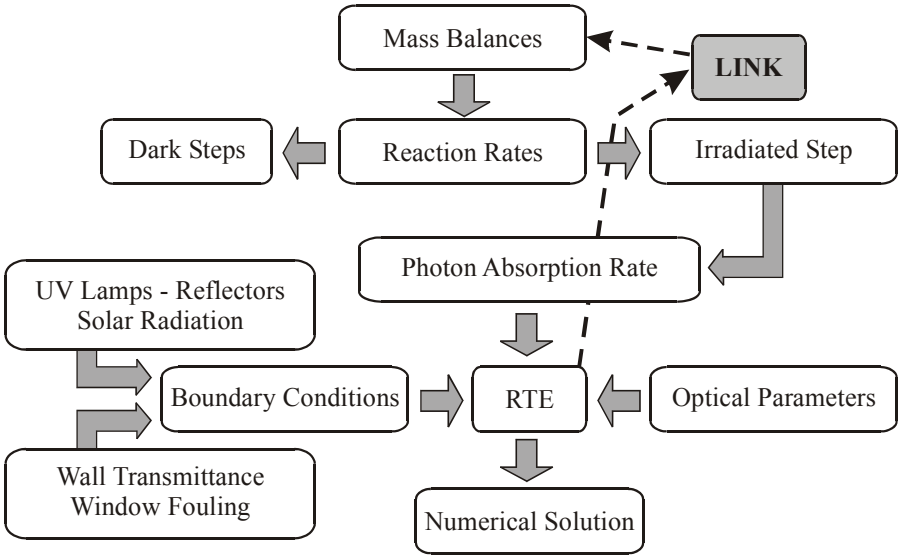

Figure 1. Evaluation of the photon absorption rate.

2. THE RADIATIVE TRANSFER EQUATION

Figure 2 (a) shows a photon distribution in directions and wavelengths (or frequencies) in an elementary volume V in space, bounded by a surface A having an outwardly directed normal n. This figure illustrates the case of photons with any directions and different wavelengths in the elementary volume. For example, white dots can represent a wavelength λ_1 and black dots a wavelength λ_2. Then, in Figure 2 (b), photons with any direction and with a single wavelength (white dots or λ_1) are exemplified. Finally, Figure 2 (c) illustrates photons with a single direction and with a single wavelength (λ_1).

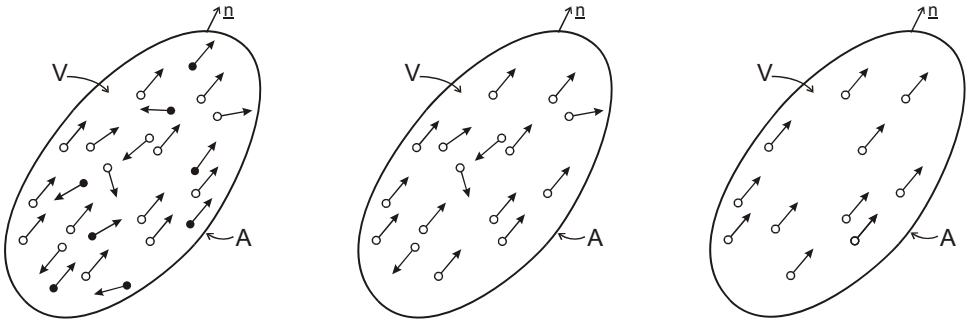

(a) (b) (c)

Figure 2. Characterization of the photon distribution in directions and wavelengths (adapted from Cassano et al., 1995)

The conceptual idea introduced by this figure sequence (Figures 2 a, b and c), allow us to define the fundamental property for characterizing the radiation field in a photochemical reactor: the **Spectral Specific Intensity**. This radiation property is defined as the amount of energy per unit time, per unit normal area, per unit solid angle, and per unit wavelength interval:

$$I_\lambda\left(\underline{x},\underline{\Omega},t\right)=\frac{dE_\lambda}{dt\,dA\cos\theta\;d\Omega\;d\lambda} \tag{1}$$

Note that the monochromatic radiation intensity is a function of position ($\underline{x}$), direction ($\underline{\Omega}$), and time (t). In photoreactor engineering, the usual units for I_λ are Einstein per square meter, per steradian, per nm, and per second.

Performing a photon balance in a fixed volume in space V, we can write (Ozisik, 1973; Cassano et al., 1995):

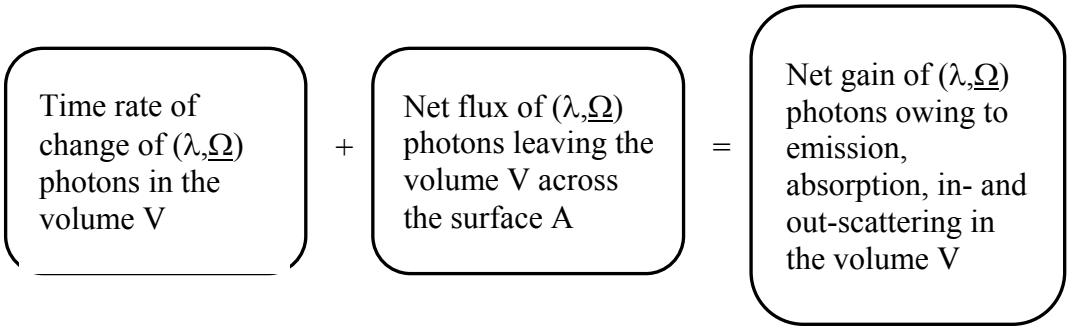

Considering the two source terms (emission and in-scattering) and the two sink terms (absorption and out-scattering) defined on the right hand side of the previous expression, one can write:

$$\frac{1}{c}\frac{\partial I_{\lambda,\underline{\Omega}}}{\partial t}+\nabla\cdot\left(I_{\lambda,\underline{\Omega}}\underline{\Omega}\right)=W^{em}_{\lambda,\underline{\Omega}}-W^{ab}_{\lambda,\underline{\Omega}}-W^{ou-s}_{\lambda,\underline{\Omega}}+W^{in-s}_{\lambda,\underline{\Omega}} \tag{2}$$

Two important assumptions can be considered in Equation (2): (i) steady state conditions of the radiation field $\left(\frac{1}{c}\frac{\partial I_{\lambda,\underline{\Omega}}}{\partial t}=0\right)$ and (ii) no radiation emission at the low working temperatures of the advanced oxidation processes $\left(W^{em}_{\lambda,\underline{\Omega}}=0\right)$. Then, taking into account the constitutive relationships for each one of the terms in Equation (2), the final expression of the RTE may be written as:

$$\frac{dI_\lambda(\underline{x},\underline{\Omega},t)}{ds} = -\underbrace{\kappa_\lambda\, I_\lambda(\underline{x},\underline{\Omega},t)}_{\text{ABSORPTION}} - \underbrace{\sigma_\lambda\, I_\lambda(\underline{x},\underline{\Omega},t)}_{\text{OUT-SCATTERING}} + \underbrace{\frac{\sigma_\lambda}{4\pi}\int_{\Omega'=4\pi} p(\underline{\Omega}'\rightarrow\underline{\Omega})\, I_\lambda(\underline{x},\underline{\Omega}',t)\, d\Omega'}_{\text{IN-SCATTERING}} \quad (3)$$

3. APPLICATION TO A NONPARTICIPATING MEDIUM

In the first application, the modeling of a multiannular photocatalytic reactor for the degradation of perchloroethylene (PCE) from contaminated air streams has been studied (Figure 3). Here the gas phase has been assumed transparent because air, PCE and water vapor do not absorb radiation in the useful wavelength range.

Thus, from Equation (3), the resulting RTE applied to this nonparticipating medium is:

$$\frac{dI_\lambda(\underline{x},\underline{\Omega},t)}{ds} = 0 \quad (4)$$

Although the medium is transparent, it is important to note that radiation absorption produced by the titanium dioxide catalytic films and by the borosilicate glass walls must be introduced in the radiation field model for this photocatalytic reactor.

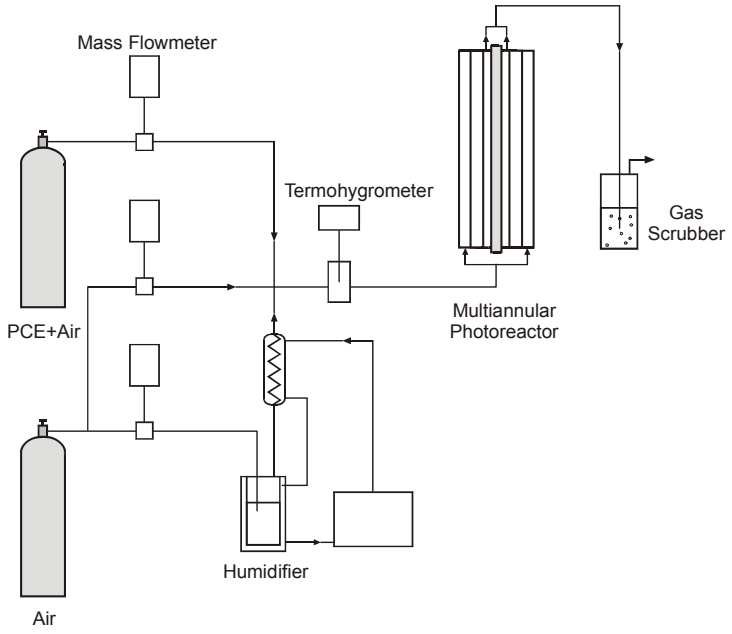

Figure 3. Flow-sheet of the experimental device (adapted from Imoberdorf et al., 2006)

3.1. Reactor Model

A radiation field model has been proposed by Imoberdorf et al. (2006) for the multiannular photocatalytic reactor. The final expression of the LSRPA at a given point (r,z) on the reactor catalytic walls is:

$$e^{a,s}(r,z)=\sum_{\lambda}\frac{P_{\lambda,L}}{2\pi^2 R_L L_L}\int_{\phi_L}\cos\phi\,d\phi\int_{\theta_L}\sin^2\theta\,d\theta\exp\left(-m_g\frac{\kappa_{\lambda,g}e_g}{\cos\gamma_n}-m_f\frac{\kappa_{\lambda,f}e_f}{\cos\gamma_n}\right)\left[1-\exp\left(-\frac{\kappa_{\lambda,f}e_f}{\cos\gamma_n}\right)\right] \quad (5)$$

In this equation, the integration over all useful wavelengths (λ) and over all ray directions (ϕ,θ) have been performed. Also, the radiation attenuation effects by the glass tube walls and the titanium dioxide films in the path of the radiation beams have been considered.

The degradation of PCE in an air stream was previously studied for different values of pollutant feed concentrations, relative humidity levels, and light intensities, using a flat-plate reactor operated under kinetic control regime (Imoberdorf et al., 2005). An expression of the intrinsic reaction kinetics was developed on the basis of a reaction scheme reported by Sanhueza et al. (1976). The following results were obtained: first order kinetics with respect to PCE concentration, linear dependence with respect to the irradiation level, and site-competitive kinetics for the dependence on the relative humidity. The reaction rate expression and the regressed kinetic parameters were:

$$\Re_{PCE}=-\alpha\frac{C_{PCE}}{1+K_w C_w}e^{a,s} \quad (6)$$

$\alpha = 1.54\times10^{8}\ \text{cm}^3\,\text{Einstein}^{-1}$ and $K_w = 3.21\times10^{-4}\ \text{m}^3\,\text{mg}^{-1}$.

For the multiannular reactor modeling, a two-dimensional mass balance can be written taking into account the LSRPA evaluated with the radiation field model (Equation 5), the intrinsic reaction rate (Equation 6), and the diffusion process of the PCE in air. The mass-transfer differential equation and the corresponding boundary conditions inside each annular space "j" are (Imoberdorf et al., 2006):

$$v_{z,j}(r)\frac{\partial C_{PCE}}{\partial z}=D_{PCE,air}\frac{1}{r}\frac{\partial}{\partial r}\left(r\frac{\partial C_{PCE}}{\partial r}\right) \qquad (j = 1, 2, 3) \quad (7)$$

$$r = R_j \qquad D_{PCE,air}\frac{\partial C_{PCE}}{\partial r}=\Re_{PCE,R_j}\left(e^{a,s}, C_{PCE}, C_w\right) \quad (8)$$

$$r = \chi_j R_j \qquad D_{PCE,air} \frac{\partial C_{PCE}}{\partial r} = \Re_{PCE,\chi_j R_j}\left(e^{a,s}, C_{PCE}, C_w\right) \tag{9}$$

$$z = z_j \qquad C^{in}_{PCE,j} = C^{ou}_{PCE,j-1} \tag{10}$$

In Equation (10), it is assumed that the inlet PCE concentration at the annular space "j" is equal to the outlet PCE concentration of the annular space "j-1".

3.2. Experiments

The multiannular photocatalytic reactor consists of four borosilicate glass tubes which are transparent to UVA radiation, with a 18 W, tubular UV lamp placed at the central axis of the system (Figure 3). The glass tube walls were coated with sol-gel TiO_2 thin films.

The reactor was fed with a mixture of PCE and air with controlled humidity and temperature. The PCE-water vapor-air stream flows trough the annular spaces, entering the reactor by the external annulus and leaving the system by the internal one. The radiation incident on the TiO_2 films can be controlled by means of a neutral density filter located between the lamp and the internal walls. The PCE concentrations in the inlet and outlet streams were determined by gas chromatography.

3.3. Results and Discussion

Table 1 shows experimental and model PCE concentrations at the reactor outlet as a function of the relative humidity (Imoberdorf et al., 2006). These runs were performed at constant volumetric flow rate (12.5 cm^3/s) and Superficial Rate of Photon Absorption (1.0×10^{-11} Einstein/cm^2 s).

Table 1. Effect of the relative humidity on the PCE concentration at the reactor outlet (*)

Relative Humidity (%)	C^{exp}_{PCE} **(mg m^{-3})**	C^{mod}_{PCE} **(mg m^{-3})**	**Error (%)**
11	34.15	33.70	1.32
30	38.75	39.39	1.65
48	40.45	42.04	3.93
89	43.55	44.93	3.17

(*) $C^{in}_{PCE} = 50$ mg m^{-3}

It can be noted that increasing the relative humidity decreases the PCE conversion (or increases the PCE concentration) at the reactor outlet. A competitive adsorption between water vapor and the PCE molecules for the active sites on the surface of the titanium dioxide has been proposed to explain this effect. Predicted pollutant concentrations show satisfactory agreement when compared with experimental results.

4. APPLICATION TO A MEDIUM WITH RADIATION ABSORPTION

In this example, the degradation of a specific organic pollutant in aqueous solution using the Fenton and photo-Fenton systems have been studied (Figure 4). The reaction was conducted in a flat-plate solar reactor placed inside a batch recycling system including a tank.

From Equation (3), the resulting RTE for this homogeneous media where there is only radiation absorption is given by:

$$\frac{dI_\lambda(\underline{x},\underline{\Omega},t)}{ds} = -\kappa_\lambda\ I_\lambda(x,\underline{\Omega},t) \tag{11}$$

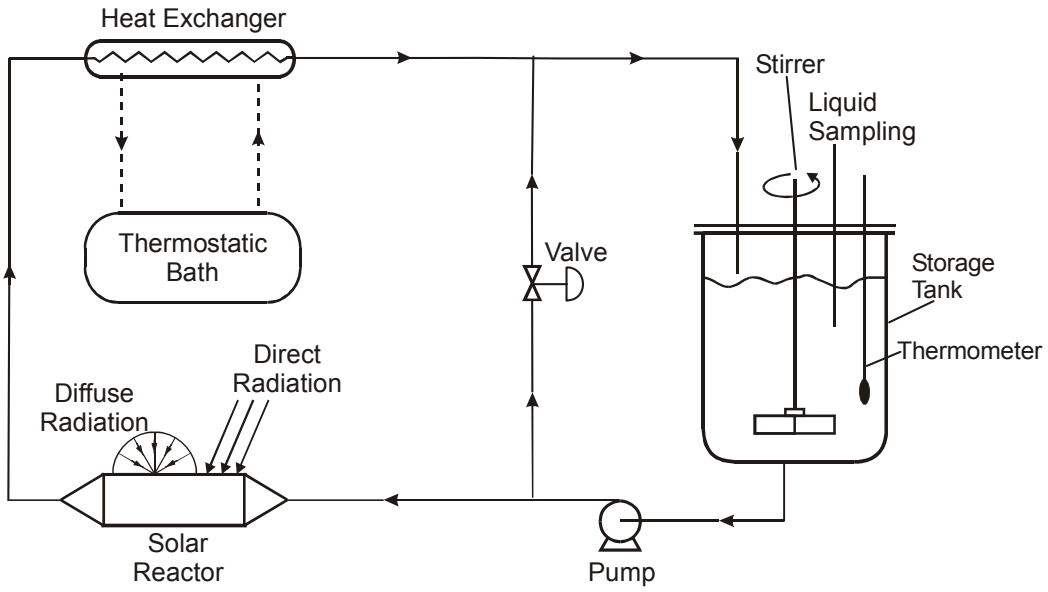

Figure 4. Experimental device (adapted from Rossetti et al., 2004)

4.1. Reactor Model

A one-dimensional radiation field model inside a nonconcentrating, flat-plate solar photoreactor has been proposed and experimentally verified with a chemical actinometer by Rossetti et al. (1998). The radiation model considers that the glass window receives direct and diffuse solar radiation. A similar expression can be applied here to compute the spectral LVRPA as a function of the spatial coordinate "x":

$$e^a_\lambda(x) = \kappa_\lambda \left\{ q_{D,\lambda} \frac{\left[1-\rho_{a-g}(\mu_i^*)\right]\left[1-\rho_{g-w}(\mu_r')\right]\tau_\lambda(\mu_r')}{1-\tau_\lambda^2(\mu_r')\,\rho_{a-g}(\mu_r')\,\rho_{g-w}(\mu_r')} \exp(-\kappa_\lambda x/\mu_r) + \right.$$
$$2q_{S,\lambda}\frac{n_w^2}{n_a^2}\int_{\mu_{cr}}^{1} \frac{\left[1-\rho_{a-g}(\mu^*)\right]\left[1-\rho_{g-w}(\mu')\right]\tau_\lambda(\mu')}{1-\tau_\lambda^2(\mu')\,\rho_{a-g}(\mu')\,\rho_{g-w}(\mu')} \exp(-\kappa_\lambda x/\mu)\,d\mu + \qquad (12)$$
$$\left. 2\rho_B q_{B,\lambda}\left[\int_0^1 \rho_{w-g}(\mu)\exp[-\kappa_\lambda(L+x)/\mu]\,d\mu + \int_0^1 \exp[-\kappa_\lambda(L-x)/\mu]\,d\mu\right]\right\}$$

Here $\mu = \cos\theta$, $\tau_\lambda = \exp(-\kappa_{g,\lambda}\, e/\mu)$, $q_{D,\lambda}$ and $q_{S,\lambda}$ are the spectral direct and diffuse (isotropic) solar radiation, $q_{B,\lambda}$ the spectral radiation flux reaching the reactor bottom, κ_λ is the spectral volumetric absorption coefficient of the absorbing species, ρ_B is the reactor bottom reflectivity, and ρ_{i-j} are the air-glass, glass-water, water-glass reflectivities.

The kinetic model for Fenton and photo-Fenton reactions was based on the reaction scheme proposed by Pignatello (1992) and De Laat and Gallard (1999). The final mathematical expressions proposed by Rossetti et al. (2002) may be used to compute the formic acid ($\Re_{FA}$) and hydrogen peroxide ($\Re_{HP}$) reaction rates:

$$\Re_{FA}(x,t) = -\left(\frac{\overline{\Phi}\sum_\lambda e^a_\lambda(x)}{1+\alpha_3(C_{HP}/C_{FA})}\right) + \left(1+\frac{\overline{\Phi}\sum_\lambda e^a_\lambda(x)}{\alpha_4 C_{Fe^{3+}} C_{HP}}\right)^{1/2} r^t_{FA}(t) \qquad (13a)$$

$$\Re^t_{FA}(t) = -\alpha_1 \frac{1+\alpha_2(C_{HP}/C_{Fe^{3+}})}{1+\alpha_3(C_{HP}/C_{FA})} C_{Fe^{3+}} C_{HP} \qquad (13b)$$

$$\Re_{HP}(x,t) = \left(\frac{\overline{\Phi}\sum_\lambda e^a_\lambda(x)}{1+\alpha_3(C_{HP}/C_{FA})}\right) + \left(1+\frac{\overline{\Phi}\sum_\lambda e^a_\lambda(x)}{\alpha_4 C_{Fe^{3+}} C_{HP}}\right)^{1/2} r^t_{HP}(t) \qquad (14a)$$

$$\Re_{HP}^{t}(t) = -\left[1 + \frac{1 + \alpha_2 \left(C_{HP}/C_{Fe^{3+}}\right)}{1 + \left(C_{FA}/\alpha_3\, C_{HP}\right)}\right] \alpha_1 C_{HP} C_{Fe^{3+}} \qquad (14b)$$

In Equations (13) and (14) $e_{\lambda}^{a}(x)$ is the LVRPA, $\overline{\Phi}$ is the wavelength averaged primary quantum yield, C_i are the formic acid (FA), hydrogen peroxide (HP), and ferric ion (Fe^{3+}) concentrations, and α_i are kinetic parameters. Both thermal and photochemical pollutant degradation rates were included in the complete kinetic expressions. Note that $\Re_{FA}^{t}$ and $\Re_{HP}^{t}$ are the thermal or Fenton formic acid and hydrogen peroxide degradation rates, respectively.

Then, for the well-stirred batch recycling solar reactor, the mass balance and the initial condition for the formic acid and hydrogen peroxide are given by (Rossetti et al., 2004):

$$\frac{dC_i}{dt} = \frac{V_R}{V_T} \left\langle \Re_i(x,t) \right\rangle_{V_R} + \left(\frac{V_{Tk}}{V_T}\right) \Re_i^{t}(t) \qquad (i = FA, HP) \qquad (15)$$

$$t = 0 \qquad C_i = C_i^0 \qquad (16)$$

where V_R, V_{Tk}, and V_T are the reactor, tank, and total liquid volumes, respectively.

4.2. Experiments

The apparatus was a flat-plate solar reactor placed inside a recycling system (Figure 4). Experimental runs were conducted at pH = 3 and three temperatures: 25, 40 and 55°C. Runs were carried out during 30 min and samples were withdrawn at equal time intervals. Prior to analysis, samples were quenched by addition of sodium sulfite. Formic acid was analyzed with TOC measurements, hydrogen peroxide with a modified iodimetric technique, and ferrous ion with spectrophotometric techniques.

4.3. Results and Discussion

Experimental and predicted formic acid concentrations after 20 min of reaction time for 25, 40 and 55 °C are illustrated in Table 2 (Farias et al., 2007). Constant values of the time-averaged solar zenith angle ($<\theta_Z>$ = 9.5°), ferric ion concentration ($C_{Fe^{3+}}$ = 1 mol m^{-3}) and hydrogen peroxide to formic acid molar ratio (C_{HP}^0/C_{FA}^0 = 3) were used. Model predictions are compared with

experimental data and a good representation of the organic pollutant concentration is observed. Notice that increasing the reaction temperature increases the formic acid conversion (or decreases the FA concentration). The significant increase of the formic acid conversion can be mainly explained by the effect of the reaction temperature on the thermal (or Fenton) reaction.

Table 2. Effect of the temperature on the formic acid concentration, t = 20 min (*)

Temperature (°C)	C_{FA}^{exp} **(mol m^{-3})**	C_{FA}^{mod} **(mol m^{-3})**	**Error (%)**
25	1.353	1.368	1.11
40	0.838	0.845	0.83
55	0.0924	0.1078	16.67

(*) C_{FA}^{0} = 2.2 mol m^{-3}

5. APPLICATION TO A MEDIUM WITH RADIATION ABSORPTION AND SCATTERING

In this case, the intrinsic kinetics of the decomposition of 4-chlorophenol (4-CP) in water was studied, using a photocatalytic slurry reactor (Figure 5). In heterogeneous photoreactors, the LVRPA evaluation is more complex due to the simultaneous existence of radiation absorption and scattering.

Thus, the complete RTE (Equation 3) must be used for this heterogeneous media:

$$\frac{dI_\lambda(\underline{x},\underline{\Omega},t)}{ds} = -(\kappa_\lambda+\sigma_\lambda)\,I_\lambda(\underline{x},\underline{\Omega},t)+\frac{\sigma_\lambda}{4\pi}\int_{\Omega'=4\pi} p(\underline{\Omega}'\rightarrow\underline{\Omega})\,I_\lambda(\underline{x},\underline{\Omega}',t)\,d\Omega' \qquad (17)$$

5.1. Reactor Model

A one-dimensional (x), one directional (θ) radiation model has been applied to this photoreactor (Satuf et al., 2007a). Monochromatic radiation intensities, $I_\lambda(x,\mu)$, can be obtained from the solution of the RTE:

$$\mu\frac{\partial I_\lambda(x,\mu)}{\partial x} = -(\kappa_\lambda+\sigma_\lambda)\,I_\lambda(x,\mu)+\frac{\sigma_\lambda}{2}\int_{-1}^{1} p(\mu,\mu')I_\lambda(x,\mu')\,d\mu' \qquad (18)$$

where $\mu=\cos\theta$ and p(μ,μ') is the phase function for scattering.

Equation (18) must be solved with the appropriate boundary conditions at both irradiated windows of the reactor (x = 0 and x = L), in terms of the radiation intensity:

$$I_\lambda(0,\mu) = I_{0,\lambda} + \Gamma_{W,\lambda}(-\mu)\, I_\lambda(0,-\mu) \qquad \mu_c \le \mu \le 1 \tag{19}$$

$$I_\lambda(0,\mu) = \Gamma_{W,\lambda}(-\mu)\, I_\lambda(0,-\mu) \qquad 0 \le \mu \le \mu_c \tag{20}$$

$$I_\lambda(L,-\mu) = I_{L_R,\lambda} + \Gamma_{W,\lambda}(\mu)\, I_\lambda(L,\mu) \qquad \mu_c \le \mu \le 1 \tag{21}$$

$$I_\lambda(L,-\mu) = \Gamma_{W,\lambda}(\mu)\, I_\lambda(L,\mu) \qquad 0 \le \mu \le \mu_c \tag{22}$$

where μ_c is the cosine of the critical angle θ_c.

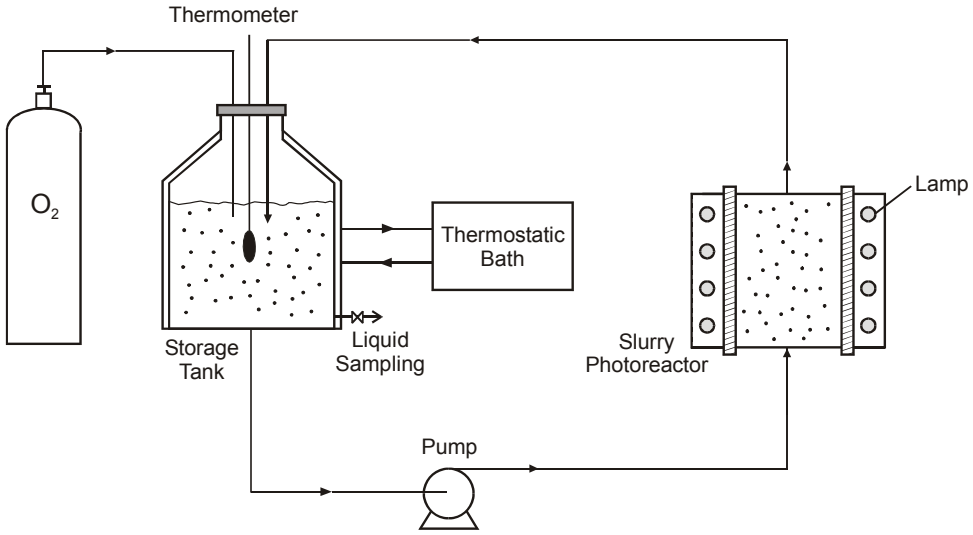

Figure 5. Experimental device (adapted from Satuf et al., 2007a).

The Discrete Ordinate Method was employed to solve Equations (18) to (22). Then, the monochromatic LVRPA can be computed by integration of the spectral radiation intensity over all possible directions (μ). Polychromatic operation may be modeled integrating the monochromatic LVRPA over the useful wavelength interval:

$$e^a(x) = 2\pi \int_\lambda \kappa_\lambda \int_{-1}^{1} I_\lambda(x,\mu)\, d\mu\, d\lambda \tag{23}$$

Values of the volumetric absorption (κ_λ) and scattering (σ_λ) coefficients as a function of the wavelength and catalyst concentration, and of the spectral

asymmetry factor of the Henyey and Greenstein phase function can be obtained from Satuf et al. (2005).

Based on a reaction sequence reported by Turchi and Ollis (1990) and Almquist and Biswas (2001), a kinetic model was proposed by Satuf et al. (2007b) for the photocatalytic degradation of 4-CP. This model also takes into account the formation and disappearance of the main intermediate products: 4-chlorocatechol (4-CC) and hydroquinone (HQ). The final kinetic expressions for this parallel-series reacting system are:

$$\Re_{4-CP,1} = \alpha_{2,1} C_{4-CP}\left(-1+\sqrt{1+\frac{\alpha_1}{a_v}e^{a}}\right) \qquad \Re_{4-CP,2} = \alpha_{2,2} C_{4-CP}\left(-1+\sqrt{1+\frac{\alpha_1}{a_v}e^{a}}\right) \tag{24}$$

$$\Re_{4-CC} = \alpha_4 C_{4-CC}\left(-1+\sqrt{1+\frac{\alpha_1}{a_v}e^{a}}\right) \qquad \Re_{HQ} = \alpha_5 C_{HQ}\left(-1+\sqrt{1+\frac{\alpha_1}{a_v}e^{a}}\right) \tag{25}$$

Here $\Re_{4-CP,1}$ is the 4-CP degradation rate to give 4-CC, $\Re_{4-CP,2}$ is the 4-CP degradation rate to give HQ, $\Re_{4-CC}$ is the 4-CC degradation rate, and $\Re_{HQ}$ is the HQ degradation rate.

The mass balance for the photocatalytic slurry reactor can be simplified on the basis of the following assumptions: (i) the system is perfectly stirred, (ii) there is a differential conversion per pass in the reactor, (iii) there are no mass transport limitations, and (iv) the chemical reaction occurs only at the solid-liquid interface. Under these assumptions, the mass balance equation and the initial condition for a generic species "i" can be written as:

$$\varepsilon_L \left.\frac{dC_i(t)}{dt}\right|_{Tk} = a_v \nu_i \frac{V_R}{V_T}\left\langle \Re(x,t)\right\rangle_{A_R} \qquad (i = 4\text{-CP, 4-CC, HQ}) \tag{26}$$

$$t = 0 \qquad C_i = C_i^0 \tag{27}$$

Solving Equations (23) to (27) we get the molar concentrations of 4-CP, 4-CC, and HQ as a function of time.

5.2. Experiments

Figure 5 provides a schematic representation of the experimental setup for the kinetic study. The reactor was operated as a perfectly mixed, isothermal device, placed inside the loop of a batch recycle system. It was made of stainless steel and Teflon, with two circular borosilicate glass windows. Irradiation was produced by two emission modules placed at both sides of the reactor. Each one of them is

formed by four UV tubular, black light lamps of 4 W. Ground glass plates, situated between the lamps and the glass windows were used to generate diffuse radiation at the wall of radiation entrance. With the aim of varying the optical thickness of the system, the reactor was constructed with a special mechanism of mobile windows to modify the reactor length.

The photocatalytic reaction was carried out in the presence of an excess of oxygen over the stoichiometric demand. The catalyst was a suspension of fine particles of Aldrich titanium dioxide. In order to obtain the values of the kinetic parameters, experimental runs were performed with the following range of values for the operating variables: (i) TiO_2 loading (0.05, 0.1, 0.5, 1.0×10^{-3} g m^{-3}), (ii) irradiation level (30, 65, 100%), and (iii) reactor length (0.5, 1.0, 5.0 cm). The initial 4-CP concentration in all experiments was 0.140 mol m^{-3} and the pH of the suspension was 2.5.

5.3. Results and Discussion

A Levenberg-Marquardt optimization algorithm was applied to estimate the kinetic parameters α_1, $\alpha_{2,1}$, $\alpha_{2,2}$, α_4, and α_5 involved in Equations (24) and (25). Values of the five kinetic parameters with the 95% confidence interval were reported by Satuf et al. (2007b).

Table 3 shows the results derived from the proposed reactor model and the regressed kinetic parameters and a comparison with the experimental data (Satuf, 2006). Concentrations of 4-CP at a reaction time of 1 hour, for different TiO_2 concentrations between 0.05 and 1.00×10^{-3} g m^{-3}, are presented. Good agreement was found between predicted and experimental results.

Table 3. Effect of the catalyst concentration on the 4-CP concentration, t = 1 h (*)

TiO_2 Concentration $\times 10^3$ (g m^{-3})	**C_{4-CP}^{exp} (mol m^{-3})**	**C_{4-CP}^{mod} (mol m^{-3})**	**Error (%)**
0.05	0.1157	0.1058	8.6
0.10	0.0975	0.0899	7.7
0.50	0.0784	0.0816	4.1
1.00	0.0590	0.0659	11.7

(*) C_{4-CP}^{0} = 0.140 mol m^{-3}

It should be noted that increasing the catalyst concentration increases the pollutant conversion (or decreases the 4-CP concentration), but this effect

becomes less significant when the TiO_2 concentration is higher than 0.50×10^{-3} g m^{-3}. After this catalyst loading the photon absorption rate reaches a maximum and beyond this catalyst concentration, no much improvement in the 4-CP degradation can be achieved.

6. CONCLUSIONS

A general methodology for photoreactor analysis and design, based on the fundamentals of chemical reaction engineering and radiative transfer in participating media has been presented. To illustrate the proposed approach, three different applications have been made in the field of Advanced Oxidation Processes. The Radiative Transfer Equation was successively applied to (i) a reaction space for a nonparticipating medium to study a photocatalytic reactor for air purification, (ii) a homogeneous medium with radiation absorption to model a homogeneous photo-Fenton solar reactor, and (iii) a heterogeneous medium with radiation absorption and scattering to obtain the kinetic parameters in a heterogeneous photocatalytic slurry reactor. This general methodology emphasizes the need of a systematic and rigorous approach to the analysis and design of homogeneous and heterogeneous photoreactors for air and water remediation.

NOTATION

A	area, cm^2
a_v	catalytic surface area per unit suspension volume, 1/cm
C	molar concentration, mol/cm^3
Cm	catalyst mass concentration, g/cm^3
c	speed of light, m/s
D_i	diffusion coefficient of species i in the mixture, cm^2/s
E	radiative energy, J
e	thickness, cm
e^a	local volumetric rate of photon absorption, Einstein/cm^3 s
$e^{a,s}$	local superficial rate of photon absorption, Einstein/cm^2 s
I	radiation intensity, Einstein/cm^2 sr s
K	equilibrium constant, m^3/mg
L	length, cm
m	number of times that a radiation beam has been attenuated by a glass or a film, dimensionless
n	refractive index, dimensionless
$\underline{n}$	unit normal vector, dimensionless
P	emission power, Einstein/ s

p	phase function, dimensionless
q	net radiative flux, Einstein/cm^2 s
$\Re$	reaction rate, mol/cm^3 s
R	radius, cm
r	radial coordinate, cm
s	linear coordinate along the direction $\underline{\Omega}$, cm
t	time, s
V	volume, cm^3
v_z	axial velocity, cm/s
W	gain or loss of energy, Einstein/cm^3 sr s
x, y, z	rectangular Cartesian coordinates, cm
$\underline{x}$	spatial position vector, cm
z	axial coordinate, cm

Greek letters

α_i	kinetic parameter
β	volumetric extinction coefficient, 1/cm
Γ	global reflection coefficient, dimensionless
γ_n	angle between the ray trajectory and the film outwardly directed normal, rad
ε_L	liquid hold-up, dimensionless
θ	spherical coordinate, rad
θ_Z	solar zenith angle, deg
κ	volumetric absorption coefficient, 1/cm
λ	radiation wavelength, nm
μ	the quantity cos θ, dimensionless
ν	stoichiometric coefficient, dimensionless
ρ	reflectivity, dimensionless
σ	volumetric scattering coefficient, 1/cm
ϕ	spherical coordinate, rad
Φ	primary quantum yield, mol/Einstein
χ	internal/external radius ratio, dimensionless
Ω	solid angle, sr
$\underline{\Omega}$	unit vector in the direction of radiation propagation

Subscripts

a	air property
B	reactor bottom property

c	relative to critical angle
D	direct radiation
FA	relative to formic acid
Fe^{3+}	relative to ferric ion
f	relative to film
g	relative to glass
HP	relative to hydrogen peroxide
HQ	relative to hydroquinone
i	relative to species i
L	relative to the lamp
L_R	relative to the reactor window at $x = L_R$
PCE	relative to perchloroethylene
R	reactor property
r	refracted radiation
S	diffuse radiation
T	total value
Tk	tank property
W	wall
w	relative to water
λ	dependence on wavelength
$\underline{\Omega}$	relative to the direction of propagation
0	relative to the reactor window at $x = 0$
$4\text{-}CC$	relative to 4-chlorocatechol
$4\text{-}CP$	relative to 4-chlorophenol

Superscripts

0	initial condition
ab	absorption
em	emission
exp	experimental
in	inlet condition
$in\text{-}s$	in-scattering
mod	model
ou	outlet condition
$ou\text{-}s$	out-scattering
t	thermal rate

Special symbol

$\langle . \rangle$	average value

$\overline{(.)}$ averaged value over the wavelength interval

REFERENCES

Almquist, C.B., Biswas, P.A., "A mechanistic approach to modeling the effect of dissolved oxygen in photo-oxidation reactions on titanium dioxide in aqueous systems", Chem. Eng. Sci., Vol. 56, 3421-3430 (2001).

Cassano, A.E., Martín, C.A., Brandi, R.J., Alfano, O.M., "Photoreactor analysis and design: Fundamentals and applications", Ind. Eng. Chem. Res., Vol. 34, 2155-2201 (1995).

De Laat, J., Gallard, H., "Catalytic decomposition of hydrogen peroxide by Fe(III) in homogeneous aqueous solution: Mechanism and kinetic modeling", Environ. Sci. Technol., Vol. 33, 2726-2732 (1999).

Farias, J., Rossetti, G.H., Albizzati, E.D., Alfano, O.M., "Solar degradation of formic acid: Temperature effects on the photo-Fenton reaction", Ind. Eng. Chem. Res., Vol. 46, 7580-7586 (2007).

Imoberdorf, G.E., Irazoqui, H.A., Cassano, A.E., Alfano, O.M., "Photocatalytic degradation of tetrachloroethylene in gas phase on TiO_2 films: A kinetic study", Ind. Eng. Chem. Res., Vol. 44, 6075-6085 (2005).

Imoberdorf, G.E., Irazoqui, H.A., Cassano, A.E., Alfano, O.M., "Modeling of a multi-annular photocatalytic reactor for PCE degradation in air", AIChE J., Vol. 52, 1814-1823 (2006).

Ozisik, M.N. "Radiative Transfer and Interactions with Conduction and Convection", Wiley, New York (1973).

Pignatello, J.J., "Dark and photoassisted Fe^{+3}-catalized degradation of chlorophenoxy herbicides by hydrogen peroxide", Environ. Sci. Technol., Vol. 26, 944-951 (1992).

Rossetti, G.H., Albizzati, E.D., Alfano, O.M., "Modeling and experimental verification of a flat-plate solar photoreactor", Ind. Eng. Chem. Res., Vol. 37, 3592-3601 (1998).

Rossetti, G.H., Albizzati, E.D., Alfano, O.M., "Decomposition of formic acid in water solution employing the photo-Fenton reaction", Ind. Eng. Chem. Res., Vol. 41, 1436-1444 (2002).

Rossetti, G.H., Albizzati, E.D., Alfano, O.M., "Modeling of a flat-plate solar reactor. Degradation of formic acid by the photo-Fenton reaction", Solar Energy, Vol. 77, 461-470 (2004).

Sanhueza, E., Hisatsune, I.C., Heiklen, J., "Oxidation of haloethylenes", Chem. Rev., Vol. 76, 801-826 (1976).

Satuf, M.L., Brandi, R.J., Cassano, A.E., Alfano, O.M., "Experimental method to evaluate the optical properties of aqueous titanium dioxide suspensions", Ind. Eng. Chem. Res., Vol. 44, 6643-6649 (2005).

Satuf, M.L., Ph.D. Dissertation, Universidad Nacional del Litoral, Santa Fe, Argentina (2006).

Satuf, M.L., Brandi, R.J., Cassano, A.E., Alfano, O.M., "Quantum efficiencies of 4-Chlorophenol photocatalytic degradation and mineralization in a well-mixed slurry reactor", Ind. Eng. Chem. Res., Vol. 46, 43-51 (2007a).

Satuf, M.L., Brandi, R.J., Cassano, A.E., Alfano, O.M., "Scaling-up of slurry reactors for the photocatalytic degradation of 4-chlorophenol", Catal. Today, Vol. 129, 110–117 (2007b).

Turchi, C.S., Ollis, D.F., "Photocatalytic degradation of organic water contaminants: mechanisms involving hydroxyl radical attack", J. Catal., Vol. 122, 178-192 (1990).